

Double cyclic variations in orbital period of the eclipsing cataclysmic variable EX Dra

Zhong-tao Han^{1,2,3} · Sheng-bang Qian^{1,2,3} · Irina Voloshina⁴ · Li-Ying Zhu^{1,2,3}

Received: 14 January 2017 / Accepted: 2 May 2017 / Published online: 30 May 2017
© Springer Science+Business Media Dordrecht 2017

Abstract EX Dra is a long-period eclipsing dwarf nova with $\sim 2\text{--}3$ mag amplitude outbursts. This star has been monitored photometrically from November, 2009 to March, 2016 and 29 new mid-eclipse times were obtained. By using new data together with the published data, the best fit to the $O - C$ curve indicate that the orbital period of EX Dra have an upward parabolic change while undergoing double-cyclic variations with the periods of 21.4 and 3.99 years, respectively. The upward parabolic change reveals a long-term increase at a rate of $\dot{P} = +7.46 \times 10^{-11} \text{ s s}^{-1}$. The evolutionary theory of cataclysmic variables (CVs) predicts that, as a CV evolves, the orbital period should be decreasing rather than increasing. Secular increase can be explained as the mass transfer between the secondary and primary or may be just an observed part of a longer cyclic change. Most plausible explanation for the double-cyclic variations is a pair of light travel-time effect via the presence of two companions. Their masses are determined to be $M_A \sin i'_A = 29.3(\pm 0.6)M_{Jup}$ and $M_B \sin i'_B = 50.8(\pm 0.2)M_{Jup}$. When the two companions are coplanar to the orbital plane of the central eclipsing pair, their masses would match to brown dwarfs.

Keywords Binaries: eclipsing · Binaries: cataclysmic variables · Stars: individual (EX Dra)

1 Introduction

To search substellar objects around white dwarf binaries are important for understanding of the interaction between companions and evolved stars (Qian et al. 2015). Recent years have been reported several successful examples for the detection of the planets around the white dwarf binaries such as QS Vir (Qian et al. 2010; Almeida and Jablonski 2011), NN Ser (Marsh et al. 2014), HU Aqr (Qian et al. 2011), (Goździewski et al. 2015) and RR Cae (Qian et al. 2012). These substellar companions are detected by measuring the variations in the observed mid-eclipse time via the presence of the third body. As the motion of the binary near the common centre of mass, the arrival eclipse time will vary periodically. This method was widely used to study other eclipsing binary systems containing a white dwarf and a red dwarf because the components are large differences in radius and luminosity (Parsons et al. 2010).

Cataclysmic variables are semi-detached binaries containing a white dwarf accreting material from a main-sequence star via Roche lobe overflow (Warner 1995). As one of the subclasses of CVs, dwarf novae show recurrent outbursts with the amplitude of 2–5 mag and short duration about a few days to weeks. Recently, several eclipsing dwarf novae were selected to detect the substellar companions and evolution by analyzing variations in orbital period. One of good examples is V2051 Oph, Qian et al. (2015) reported that it has a giant planet with a mass of $7.3(\pm 0.7)M_{Jup}$ and an eccentricity of $e' = 0.37$. Moreover, the secular decrease in orbital period of V2051 Oph suggested that magnetic braking may not entirely cease in fully convective stars.

✉ Z.-t. Han
zhongtaohan@ynao.ac.cn

¹ Yunnan Observatories, Chinese Academy of Sciences (CAS), P.O. Box 110, 650216 Kunming, China
² Key Laboratory of the Structure and Evolution of Celestial Objects, Chinese Academy of Sciences, P.O. Box 110, 650216 Kunming, China
³ University of Chinese Academy of Sciences, Yuquan Road 19#, Sijingshang Block, 100049 Beijing, China
⁴ Sternberg Astronomical Institute, Moscow State University, Universitetskij prospect 13, Moscow 119992, Russia

EX Dra is a long-period ($P = 5.04$ h) dwarf nova with very deep eclipse with 1.5 mag in quiescence. It was discovered in the Hamburger Quasar Survey (Bade et al. 1989). Follow-up observations by Barwig et al. (1993) showed that EX Dra is a deeply eclipsing dwarf nova with an orbital period of just over 5 h. Fiedler et al. (1997) presented spectroscopic and photometric observations, and estimated some basic parameters. By using photometric observations, Baptista et al. (2000) found that this system has a mass ratio $q = 0.72$ and an inclination $i = 85^\circ$, and that the $O - C$ diagram showed a periodic oscillation with a period of 4 yr and an amplitude of 1.2 min. Shafter and Holland (2003) analyzed the eclipse profile of multi-colour light curves with a parameter-fitting model. They derived a mass ratio $q < 0.81$ and an inclination of $i > 83^\circ$. The revised ephemeris showed a cyclical variation with a period of 5 yr. Recently, the analysis by Pilarčik et al. (2012) given a period modulation with a period of 21 yr and an amplitude of 2.5 min.

In present paper, we use new eclipse timings coupled with the old data to analyse the $O - C$ diagram of EX Dra. Our results indicated that both there are two possible brown dwarfs orbiting EX Dra, and this star may be undergoing a peculiarly evolutionary stage.

2 CCD photometric observations and new mid-eclipse times

We started to monitor EX Dra since 09, November 2009 by using the 0.6-m reflecting telescope attached an Andor DV436 2K CCD camera at the Yunnan Observatories (YNAO). Later, this star was monitored with the 85-cm telescope mounted an Anor DW436 1K CCD camera at the XingLong station of the National Astronomical Observatories and the 2.4-m telescope at the Lijiang observational station in YNAO. Since the May of 2014, EX Dra was continuously observed with CCD photometer on 50-cm (Apogee Alta U8300 with 528×512 pixels) and 60-cm (Apogee 47, field 1024×1024 pixels) telescopes of Sternberg Astronomical Institute Crimean Station in R-band. Four light curves of EX Dra in quiescence are displayed in Fig. 1. The phases were computed by using the linear ephemeris,

$$Min.I = HJD2456065.154955 + 0.209937316 \times E, \quad (1)$$

where HJD2456065.154955 is the initial epoch from our mid-eclipse times listed in Table 1, and 0.209937316 d is the orbital period from Pilarčik et al. (2012). The most obvious features in Fig. 1 are that the light curves in quiescence exhibit double eclipse rarely and strong orbital hump. In addition, the shape and brightness are variable with time. This can be explained as the change of mass transfer rate and the instability of accretion disc. The egress of white

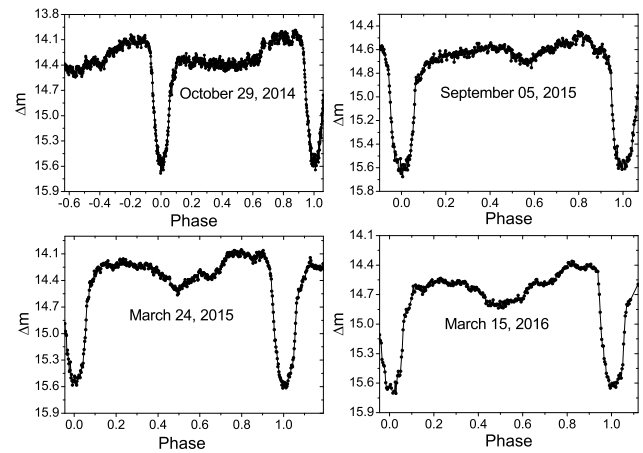


Fig. 1 Four eclipsing light curves of EX Dra observed by using the 60 cm telescope in Sternberg Astronomical Institute Crimean Station

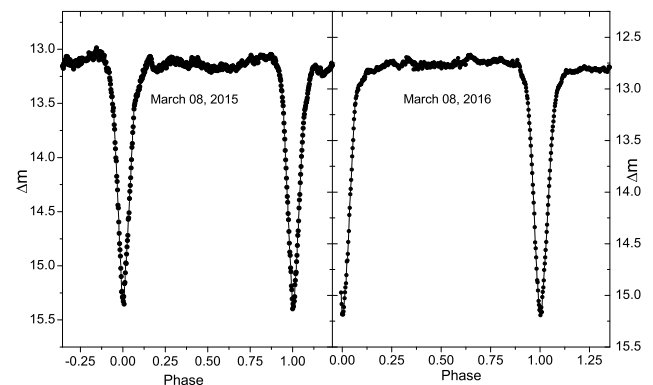


Fig. 2 Two eclipse profiles of EX Dra during outbursts obtained with 60 cm telescope in Sternberg Astronomical Institute Crimean Station on 2015 March 08 and 2016 March 08, respectively

dwarf can be seen clearly in the light curves. For comparison, two profiles during outburst are shown in Fig. 2. These curves are V-shaped and symmetric, indicating an axisymmetrical brightness distribution in the accretion disc at maximum. The orbital hump disappears during outburst.

By adopting the same method from Pilarčik et al. (2012), the 29 new mid-eclipse times during quiescence were obtained and listed in Table 1. We only used the light curves during quiescence to determine the mid-eclipse times. The reason also has been discussed in Pilarčik et al. (2012). This consistency with previous published eclipse timings highly increases reliability of the following analysis. We also computed the eclipse width of the white dwarf as $\Delta\tau = 0.0230(1)$ days, which is very close to previous studies. The uncertainty in determining mid-eclipse times depends on the time resolution and signal to noise ratio. We estimate that the error of mid-eclipse times is about quarter of the integration time. The reason is that the errors of mid-egress and mid-ingress times are about half of the time resolution, and the mid-eclipse times are average value of the mid-ingress and

Table 1 New CCD mid-eclipse times of EX Dra in quiescence

Min. (HJD)	Min. (BJD)	E	$O - C$	Errors	Exp.time (s)	Filters	Telescopes
2455144.9992	2455144.9999	12719	0.0021	0.0002	60	R	0.6 m
2455746.0491	2455746.0498	15582	0.0014	0.0001	40	R	85 cm
2456065.1550	2456065.1557	17102	0.0026	0.0002	60	N	2.4 m
2456523.0282	2456523.0290	19283	0.0026	0.0001	40	I	85 cm
2456799.3056	2456799.3063	20599	0.0024	0.0001	40	R	50 cm
2456807.2833	2456807.2841	20637	0.0026	0.0001	40	R	60 cm
2456819.4599	2456819.4607	20695	0.0028	0.0001	40	R	50 cm
2456833.3160	2456833.3167	20761	0.0030	0.0001	40	R	50 cm
2456834.3655	2456834.3663	20766	0.0028	0.0001	40	R	60 cm
2456838.3540	2456838.3548	20785	0.0025	0.0001	40	R	60 cm
2456960.3272	2456960.3280	21366	0.0022	0.0004	75	R	60 cm
2456960.5372	2456960.5379	21367	0.0022	0.0004	75	R	60 cm
2457024.1480	2457024.1488	21670	0.0020	0.0004	75	R	60 cm
2457080.2018	2457080.2026	21937	0.0026	0.0002	60	R	60 cm
2457098.2561	2457098.2569	22023	0.0023	0.0002	60	R	60 cm
2457106.2335	2457106.2342	22061	0.0020	0.0001	40	R	60 cm
2457106.4443	2457106.4451	22062	0.0029	0.0001	40	R	60 cm
2457108.3340	2457108.3347	22071	0.0031	0.0001	40	R	60 cm
2457118.4105	2457118.4112	22119	0.0026	0.0001	40	R	60 cm
2457123.2390	2457123.2398	22142	0.0026	0.0001	40	R	60 cm
2457123.4493	2457123.4501	22143	0.0029	0.0001	40	R	60 cm
2457124.4968	2457124.4976	22148	0.0008	0.0001	40	R	60 cm
2457267.2561	2457267.2569	22828	0.0027	0.0001	40	R	60 cm
2457267.4668	2457267.4676	22829	0.0034	0.0001	40	R	60 cm
2457268.3058	2457268.3066	22833	0.0028	0.0002	60	R	60 cm
2457271.2457	2457271.2465	22847	0.0035	0.0002	60	R	60 cm
2457271.4561	2457271.4568	22848	0.0039	0.0001	40	R	60 cm
2457463.3380	2457463.3388	23762	0.0032	0.0001	40	R	60 cm
2457463.5479	2457463.5487	23763	0.0032	0.0001	40	R	60 cm

mid-egress times. Therefore, the errors of mid-eclipse times were determined as the combination of the errors of mid-egress and mid-ingress by using the error propagation function. All new mid-eclipse times have been converted into the *BJD* system and are listed in the second column of Table 1, corresponding to errors are also given in fifth column. The exposure time for each mid-eclipse times was listed in sixth column. The details of the used filters could be found in seventh column where “R” and “I” refer to R-band and I-band, respectively. “N” indicates that no filters were used. “0.6 m”, “85 cm” and “2.4 m” in the eighth column of the table refer to the 0.6 m, 85-cm and 2.4-m telescopes in China, while “50 cm” and “60 cm” refer to the 50-cm and 60-cm telescopes in Russia.

3 The changes of the $O - C$ curve of EX Dra

Baptista et al. (2000) shown a cyclical behaviour in $O - C$ diagram with a period of 4 years and a amplitude of

1.18 min. Follow-up studies by Shafter and Holland (2003) pointed out the period and amplitude are about 25% bigger than the corresponding values from Baptista et al. (2000). Recently, Pilarčik et al. (2012) revised ephemeris by adding many mid-eclipse times and found a greater cyclical variation with a period of 21 years and an amplitude of 2.5 min, but a singly sinusoidal ephemeris cannot describe the complex $O - C$ change well. Therefore, it seems that there are two cyclic variations in the $O - C$ diagram.

Combining new data with the old timings from the literature (Fiedler et al. 1997; Baptista et al. 2000; Shafter and Holland 2003; Pilarčik et al. 2012), the latest $O - C$ diagram was obtained (see Fig. 3). All $O - C$ values were calculated with the linear ephemeris published by Pilarčik et al. (2012),

$$Min.I = BJD2452474.80513 + 0.209937316 \times E, \quad (2)$$

where BJD2452474.80513 is the initial epoch. New $O - C$ curve is more complex than meets the eye. Based on previous studies, we suspected the existence of two cyclic variations. To describe the overall trend of the $O - C$ curve

Table 2 Parameters of the best fitting for $O - C$

Parameters	Values	
Correction on the initial epoch, ΔT_0 (d)	$-6.0(\pm 1.6) \times 10^{-4}$	
Correction on the initial period, ΔP_0 (d)	$+3.09(\pm 0.28) \times 10^{-8}$	
Rate of the linear increase, β (d/cycle)	$+1.57(\pm 0.26) \times 10^{-11}$	
Parameters	Case A	Case B
Semi-amplitude, K_A, K_B (d)	$1.04(\pm 0.24) \times 10^{-3}$	$5.80(\pm 0.73) \times 10^{-4}$
Orbital period, P_A, P_B (yr)	$21.40(\pm 1.44)$	$3.99(\pm 0.11)$
The orbital phase, φ_A, φ_B (deg)	$11.17(\pm 0.86)$	$-146.57(\pm 5.26)$

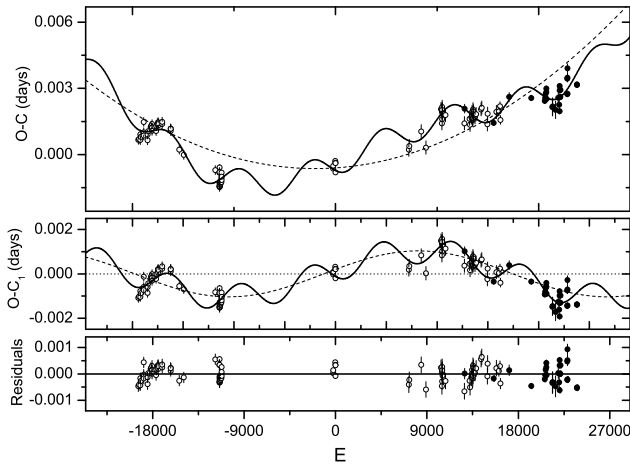


Fig. 3 $O - C$ diagrams of EX Dra with respect to the double-cyclic variations. The *open circles* and *solid circles* denote the data in literature and in our observation, respectively. The *solid line in the upper panel* refers to a combination of a upward parabolic and two cyclic changes. The *dashed line* represents only the upward parabolic variation that reveals a continuous increase in the orbital period. When the long-term period increase was subtracted, the superposition of a long (the *dashed line*) and a short (the *solid line*) periodic variation are displayed in the *middle panel*. These variations were removed, the residuals are plotted in the *lowest panel*

well, a quadratic ephemeris is required. Thus, a possible model with an upward parabolic variation and double periodic terms is considered:

$$O - C = \Delta T_0 + \Delta P_0 E + \frac{\beta}{2} E^2 + \tau_A + \tau_B, \quad (3)$$

where τ_A and τ_B are the two cyclic changes. Our best fit to the $O - C$ diagram by using the Levenberg-Marquardt method shows that both of τ_A and τ_B are strictly periodic, i.e.

$$\tau_A = K_A \sin\left(\frac{2\pi}{P_A} E + \varphi_A\right), \quad (4)$$

and

$$\tau_B = K_B \sin\left(\frac{2\pi}{P_B} E + \varphi_B\right). \quad (5)$$

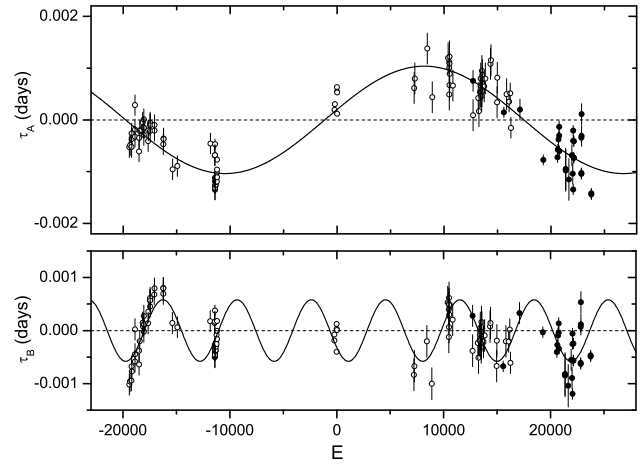


Fig. 4 The two cyclic variations τ_A and τ_B extracted from the middle panel of Fig. 3

In general, the eccentricity should be taken into account in the fitting process. However, the eccentricity was close to zero ($e < 0.01$) but with a larger error, which is why we set $e = 0$ in the final fit. All fitting parameters and the corresponding values are given in Table 2. The best-fitting results reveal a secular period increase at a rate of $\dot{P} = +7.46 \times 10^{-11} \text{ s s}^{-1}$. In Fig. 3, the dashed line in the upper panel refers to the linear period increase and the solid line represents the combination of two cyclic changes and the linear increase. After the long-term increase was subtracted, the superposition of a long (the dashed line) and a short (the solid line) periodic variation are displayed in the middle panel. Following both the linear increase and the two cyclic changes were removed, the residuals are plotted in the lowest panel. The two cyclic variations extracted from the middle panel of Fig. 3 are displayed in Fig. 4 where the periods of τ_A and τ_B are 21.40 years and 3.99 years and the corresponding amplitudes are 89.6 s and 50.1 s. The derived period modulations are very close to the previous results detected by Pilarčık et al. (2012) and Baptista et al. (2000), respectively.

4 Discussion

The standard model predicts that the evolution of CVs is driven by angular momentum losses (AMLs). The result is that, as a CV evolves, the orbital period decreases. However, our result show that the period of EX Dra is increasing at a rate of $\dot{P} = +7.46 \times 10^{-11} \text{ s s}^{-1}$. EX Dra is a long-period ($P = 5.04 \text{ h}$) CV containing a late-type main sequence star overflowing its Roche lobe ($M_2 \sim 0.54 M_\odot$) and a white dwarf ($M_1 \sim 0.75 M_\odot$) (Baptista et al. 2000), the mass transfer between two components will cause the orbit expansion. Supposing a conservation mass transfer on long time scales and adopting the parameters given by Baptista et al. (2000), a calculation using the equation (Thomas 1977)

$$\frac{\dot{P}}{P} = -3\dot{M}_2 \times \left(\frac{1}{M_1} - \frac{1}{M_2} \right), \tag{6}$$

leads to a mass transfer rate of $\dot{M}_2 = 8.34 \times 10^{-8} M_\odot \text{ yr}^{-1}$. It is alternatively possible that the quadratic term is only a part of a longer cyclic oscillation.

Our results also reveal that there are two cyclic variations in the $O - C$ curve. To interpret cyclic period changes of EX Dra, two main mechanisms are the solar-type magnetic activity cycle in M-type secondary star (Applegate 1992) and the light time travel effect. The Applegate mechanism built on the basis of the conclusion presented by Hall (1989). They found that all cool component stars are strictly limited in the spectral types later than F5. Recently, however, a statistical investigation for the cyclic period oscillations has shown that the percentages of cyclic variations for both late-type and early type interacting binaries are very close (Liao and Qian 2010). Thus, the conclusion proposed by Hall (1989) may be not correct, and moreover, Applegate (1992) already noted that his model should be revised if the shell becomes a significant fraction of the star’s mass ($M_s > 0.1 M_2$). The secondary star in EX Dra is a late-type main sequence star with the spectral type about M1-3/5 (Ritter and Kolb 2003) (update RKcat7.23 version, 2015), this star should have a very deep convective envelope. With the theoretical model calculation and statistics, the shell mass of EX Dra’s donor was estimated to be $M_s \approx 0.15 M_\odot \approx 0.28 M_2$. To explain the cyclic oscillation of the pre-CV NN Ser, moreover, Brinkworth et al. (2006) by comparing the energies required to cause the observed variation found that NN Ser’s secondary star cannot provide enough energy to drive Applegate mechanism. Using the same method for EX Dra, the required energies to produce two cyclic oscillations were calculated and shown in Fig. 5. The results show that the required minimum energy in Case A are larger than the total energy radiated in 21.4 yr, and in Case B the required minimum energy are also slightly larger than the total energy radiated in a whole cycle (see Fig. 5). Combining the

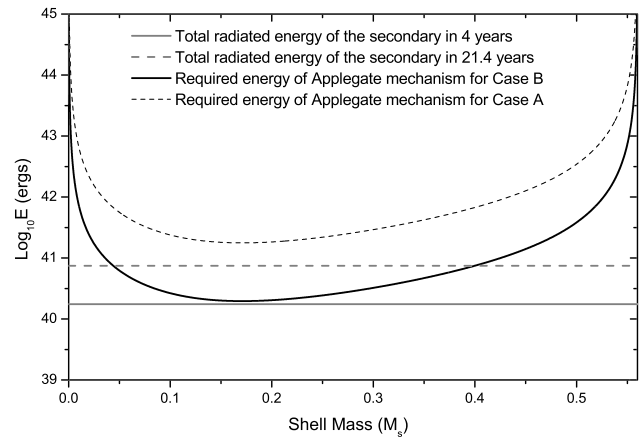


Fig. 5 Energy required to cause two periodic changes in the $O - C$ diagram by using Applegate’s mechanism. M_s refers to the assumed shell mass of the secondary star. The black dashed line denotes the energy required for different shell mass in Case A, and the black solid line corresponding to Case B. The grey solid line represents the total energy radiates from the secondary in 4 years and the grey dashed line is the total radiant energy of the secondary in 21.4 years

parameters presented by Baptista et al. (2000) with Kepler’s third law

$$P_{orb}^2 = \frac{4\pi^2 a^3}{G(M_1 + M_2)}, \tag{7}$$

to yield the orbital separation as $a = 1.62 R_\odot$. Applying $T_2 = 3400 \text{ K}$ for the M2-3 type, the luminosity of the secondary star can be draw as $L_2 = \left(\frac{R_2}{R_\odot}\right)^2 \left(\frac{T_2}{T_\odot}\right)^4 L_\odot$. Therefore, the Applegate mechanism is difficult to explain the observed cyclic changes. The most plausible explanation seems to be a pair of light travel time effects via the presence of two companions.

The mass function and the mass of tertiary companions were derived by using the following equation (Pringle and Wade 1985):

$$f(m)_A = \frac{4\pi^2}{G P_A^2} (a'_A \sin i'_A)^3 = \frac{(M_A \sin i'_A)^3}{(M_1 + M_2 + M_A)^2}, \tag{8}$$

and

$$f(m)_B = \frac{4\pi^2}{G P_B^2} (a'_B \sin i'_B)^3 = \frac{(M_B \sin i'_B)^3}{(M_1 + M_2 + M_B)^2}, \tag{9}$$

where G is the gravitational constant, P_A and P_B are the periods of τ_A and τ_B , and $a'_A \sin i'_A$ and $a'_B \sin i'_B$ can be determined by

$$a'_A \sin i'_A = K_A \times c, \tag{10}$$

and

$$a'_B \sin i'_B = K_B \times c, \tag{11}$$

Table 3 Orbital parameters of the circumbinary substellar objects

Parameters	Companion A	Companion B
Eccentricity, e_A and e_B	0	0
Mass function, $f(m)_A$ and $f(m)_B$ (M_\odot)	$1.28(\pm 0.63) \times 10^{-5}$	$6.37(\pm 0.33) \times 10^{-5}$
The companion masses, $M_A \sin i'_A$ and $M_B \sin i'_B$ (M_{Jup})	29.3(± 0.6)	50.8(± 0.2)
Semi-major axis of the planet, d_A and d_B (au, $i' = 90^\circ$)	9.83(± 1.21)	3.18(± 0.11)

K_A and K_B are the semi-amplitude of τ_A and τ_B . The results are listed in Table 3. Assuming a random distribution of orbital plane inclinations, the orbital inclination for the companion A (i.e. Case A) is larger than $22^\circ.96$, the mass corresponds to $M_A \leq 0.075 M_\odot$, it may be a brown dwarf with 74.5% and a low-mass star with only 25.5% probability. As for companion B (corresponding to Case B), if its orbital inclination is less than $42^\circ.39$, the mass is $M_B \geq 0.075 M_\odot$, it may be a brown dwarf with 52.9% and low-mass star with 47.1%. If they are coplanar (i.e. $i' = i = 85^\circ$) to the orbital plane of the eclipsing pair, their masses would match to two brown dwarfs.

5 Conclusions

We have published 29 new mid-eclipse times of EX Dra in quiescence spanning from 2009 to 2016. These mid-eclipse times were used to analyze the orbital period variation. Besides a secular increase with a rate of $\dot{P} = +7.46 \times 10^{-11} \text{ s s}^{-1}$, the orbital period also shows the double-cyclic changes. According to the evolutionary theory of CVs, the orbital period should decrease. If the long-term period increase was explained as the mass transfer from the secondary to primary star, the derived mass transfer rate is $\dot{M}_2 = 8.34 \times 10^{-8} M_\odot \text{ yr}^{-1}$. However, it is possible that the quadratic term may be just a observed part of a longer cyclic oscillation. For double periodic oscillations, EX Dra's secondary star can not provide enough energy to satisfy the energy requirements of Applegate mechanism. The more acceptable explanation is the existence of a pair of substellar objects around EX Dra. Assuming the circumbinary objects to be in the orbital plane ($i' = i = 85^\circ$) of the eclipsing pair, they are two brown dwarfs.

The orbital parameters of the substellar objects in Table 3 reveal some interesting features. First, both the orbits are circular. Second, the orbital periods of $21.40(\pm 1.44)$ and $3.99(\pm 0.11)$ years are nearly the ratio of 5 : 1. This implies that the possibility exists for the mean-motion resonance between the two companions and their orbits would be stable. From the evolutionary perspective, CVs are products of a common envelope (CE) phase (Ivanova et al. 2013). The circumbinary companions may originate from a large protoplanetary disc or a fragmentation of protostellar disc. In the former case, the formation process is similar to two hot

subdwarf stars HW Vir and AA Dor (Rauch 2000; Heber 2009), and its description will not be repeated here. In the latter case, the formation process is as follows: the objects will started with the mass a few M_{Jup} and then increase their mass by accreting material from the disc (Attwood et al. 2009; Stamatellos and Whitworth 2009a). For the former formed objects, they would migrate inwards and gain enough mass to become stars (Stamatellos et al. 2007); for the objects staying in the outer disc region, they could not gain enough mass, and become brown dwarfs (Stamatellos and Whitworth 2009b). The higher-mass objects of the inner region will evolve to progenitor of the post-common envelope binaries. The circumbinary companions formed at the almost same as their hosts and survived the CE phase (Bear and Soker 2014). Besides, there are also other possibilities, such as the second generation substellar originated in CE event (Völschow et al. 2014). However, there is only a remote possibility for EX Dra because THE substellar objects have relatively large mass (29.3 and $50.8 M_{Jup}$) (Bear and Soker 2014). Moreover, the circular orbits means that they may have existed for a long time-scales before the CE phase. Certainly, in order to confirm our conclusion, further observations are needed in the future.

Acknowledgements This work is supported by the Chinese Natural Science Foundation (Grant No. 11325315, 11133007, 11573063 and 11611530685), the Strategic Priority Research Program ‘‘The Emergence of Cosmological Structure’’ of the Chinese Academy of Sciences (Grant No. XDB09010202) and the Science Foundation of Yunnan Province (Grant No. 2012HC011). This study is also supported by the Russian Foundation for Basic Research (project No. 17-52-53200). New CCD photometric observations of EX Dra were obtained with the 60 cm and the 2.4 m telescopes at the Yunnan Observatories, the 85 cm telescope in Xinglong Observation base in China and 50 cm and 60 cm telescopes of Sternberg Astronomical Institute Crimean Station. Finally, we thank the anonymous referee for those helpful comments and suggestions.

References

- Almeida, L.A., Jablonski, F.: The Astrophysics of Planetary Systems: Formation, Structure, and Dynamical Evolution, vol. 276, p. 495 (2011)
- Applegate, J.H.: *Astrophys. J.* **385**, 621 (1992)
- Attwood, R.E., Goodwin, S.P., Stamatellos, D., Whitworth, A.P.: *Astron. Astrophys.* **495**, 201 (2009)
- Bade, N., Hagen, H.-J., Reimers, D.: In: Two Topics in X-Ray Astronomy, Volume 1: X Ray Binaries. Volume 2: AGN and the X Ray Background, vol. 296, p. 883 (1989)

- Baptista, R., Catalán, M.S., Costa, L.: *Mon. Not. R. Astron. Soc.* **316**, 529 (2000)
- Barwig, H., Fiedler, H., Reimers, D., Bade, N.: In: vanWoerden, H. (ed.) *Compact Stars in Binary Systems. Abstracts of IAU Symp.*, vol. 165, p. 89 (1993)
- Bear, E., Soker, N.: *Mon. Not. R. Astron. Soc.* **444**, 1698 (2014)
- Brinkworth, C.S., Marsh, T.R., Dhillon, V.S., Knigge, C.: *Mon. Not. R. Astron. Soc.* **365**, 287 (2006)
- Fiedler, H., Barwig, H., Mantel, K.H.: *Astron. Astrophys.* **327**, 173 (1997)
- Goździewski, K., Slowikowska, A., Dimitrov, D., et al.: *Mon. Not. R. Astron. Soc.* **448**, 1118 (2015)
- Hall, D.S.: *Space Sci. Rev.* **50**, 219 (1989)
- Heber, U.: *Annu. Rev. Astron. Astrophys.* **47**, 211 (2009)
- Ivanova, N., Justham, S., Chen, X., et al.: *Astron. Astrophys. Rev.* **21**, 59 (2013)
- Liao, W.-P., Qian, S.-B.: *Mon. Not. R. Astron. Soc.* **405**, 1930 (2010)
- Marsh, T.R., Parsons, S.G., Bours, M.C.P., et al.: *Mon. Not. R. Astron. Soc.* **437**, 475 (2014)
- Parsons, S.G., Marsh, T.R., Copperwheat, C.M., et al.: *Mon. Not. R. Astron. Soc.* **407**, 2362 (2010)
- Pilarčík, L., Wolf, M., Dubovský, P.A., Hornoch, K., Kotková, L.: *Astron. Astrophys.* **539**, A153 (2012)
- Pringle, J.E., Wade, R.A.: *Interacting Binary Stars* p. 77. Cambridge University Press, Cambridge (1985)
- Qian, S.-B., Liao, W.-P., Zhu, L.-Y., et al.: *Mon. Not. R. Astron. Soc.* **401**, L34 (2010)
- Qian, S.-B., Liu, L., Liao, W.-P., et al.: *Mon. Not. R. Astron. Soc.* **414**, L16 (2011)
- Qian, S.-B., Liu, L., Zhu, L.-Y., et al.: *Mon. Not. R. Astron. Soc.* **422**, L24 (2012)
- Qian, S.B., Han, Z.T., Fernández Lajús, E., et al.: *Astrophys. J. Suppl. Ser.* **221**, 17 (2015)
- Rauch, T.: *Astron. Astrophys.* **356**, 665 (2000)
- Ritter, H., Kolb, U.: *Astron. Astrophys.* **404**, 301 (2003)
- Shafter, A.W., Holland, J.N.: *Publ. Astron. Soc. Pac.* **115**, 1105 (2003)
- Stamatellos, D., Whitworth, A.P.: *Mon. Not. R. Astron. Soc.* **392**, 413 (2009a)
- Stamatellos, D., Whitworth, A.P.: *Mon. Not. R. Astron. Soc.* **400**, 1563 (2009b)
- Stamatellos, D., Hubber, D.A., Whitworth, A.P.: *Mon. Not. R. Astron. Soc.* **382**, L30 (2007)
- Thomas, H.-C.: *Annu. Rev. Astron. Astrophys.* **15**, 127 (1977)
- Völschow, M., Banerjee, R., Hessman, F.V.: *Astron. Astrophys.* **562**, A19 (2014)
- Warner, B.: *Cataclysmic Variable Stars* p. 28. Cambridge University Press, Cambridge (1995)